Siderophile Element Concentrations and Os Isotopic Compositions Applied to Tracing the Origins of Gold Nuggets

Braden Lense

Advisors: Dr. Richard Walker, Dr. Richard Ash

Department of Geology, University of Maryland College Park, MD, 20724

Geol 394

April 27, 2021

Abstract

The formation of gold nuggets found in alluvial deposits remains poorly understood. To assess this, the concentrations of siderophile element abundances (siderophile elements analyzed: P, V, Cr, Fe, Co, Ni, Cu, Ga, Ge, As, Mo, Mo, Ru, Rh, Pd, Ag, W, Re, Os, Ir, Pt), and $^{187}Os/^{188}Os$ ratios for samples of alluvium-associated gold nuggets from placer deposits in Costa Rica and British Columbia, have been determined.

Radiogenic ^{187}Os, is derived from the decay of ^{187}Re. The $^{187}Os/^{188}Os$ ratio is therefore a powerful tool for distinguishing between mantle and crustal rocks, due to differences in the partitioning of Re and Os within these reservoirs. This ratio of $^{187}Os/^{188}Os$ within the gold nuggets was the focus of this study and the primary geochemical tracer used to determine source lithology.

The gold nuggets in this study were found to have a several micron thick layer on the surface, which was heavily enriched in some siderophile elements compared to the interior of the nuggets. It was determined that the concentration of the surface coating, while comparatively enriched in some siderophile elements, was not high enough to warrant analyzing the surface and interior separately.

The absolute and relative abundances of the siderophile elements measured in bulk nuggets were highly variable and currently uninterpretable. Most $^{187}Os/^{188}Os$ ratios measured in this study were broadly chondritic. Three nuggets have more radiogenic signatures (0.393, 0.674, and 0.732). $^{187}Re/^{188}Os$ ratios vary considerably (0.8-520). All of the nuggets with radiogenic $^{187}Os/^{188}Os$ ratios also have high $^{187}Re/^{188}Os$ ratios. This is possible evidence that the Os in the nuggets was derived from source rocks with low Re/Os, ranging in age 40-60 Ma. With this in mind, 6 of the 7 Costa Rican nuggets are plausibly derived from gabbros or unexposed ophiolitic ultramafic rock in the Nicoya complex. The 3 British Columbian nuggets are consistent with derivation from young ultramafic rock present in the Cache Creek Group.

TABLE OF CONTENTS

Introduction

Formation of Gold Nuggets

Native gold is found in a variety of geological environments and can form through a variety of mechanisms. Studies have determined that native gold can be present in volcanic rocks (Sisson, 2003), as a precipitate in siliceous hydrothermal systems (Zhu et al. 2011), and in mafic intrusive rocks (Walker et al., 2007). However, the most abundant source of gold is alluvial gold, the ultimate source of which has been left largely unexplained.

For gold to form alluvial nuggets, it needs to be eroded out of its source rock, then concentrated into a nugget, then finally emplaced in alluvial deposits. To form larger gold nuggets, it has been theorized that sedimentary recycling needs to occur, meaning that multiple cycles of deposition and re-erosion of gold in rocks will slowly concentrate gold out of source rocks and into nuggets over geologic timescales (Youngson & Craw, 1992). Uplift is needed for the erosional processes which drive nugget formation to occur, tectonism is generally the source of this uplift. This tectonism distorts the rock record removing evidence of recycling activity only leaving the syn-tectonic environment preserved in the rock record (Youngson & Craw, 1992). Without tectonism, the gold would not to be concentrated into nuggets, though it distorts the geologic record that is needed to understand the processes which concentrated the gold into nuggets.

A proposed source of the gold composing alluvial gold nuggets are gold micronuggets found in volcanic rocks (Sisson, 2003). Though, these volcanic nuggets are much smaller (~0.75μm diameter) than any of the gold nuggets (~1cm diameter) being analyzed in this study. The jump from micronuggets to placer gold nuggets requires a sufficient mechanism to concentrate the micronuggets together to form the larger gold nuggets. There is still a disconnect between the source of the gold and the mechanism concentrating the gold. In the case of this proposed source, the source of the gold is accounted for, the factor mobilizing the gold is explained, being erosional processes, but it is lacking a mechanism for concentrating the gold from micronuggets into larger nuggets.

The precipitation of gold nuggets during serpentinization has also been proposed as a mechanism of formation. This has been theorized to be analogous to the formation of many Alaskan platinum group element nuggets, which are found to contain olivine and clinopyroxene inclusions. Serpentinization is a process in which hydrothermal fluid alters ultramafic rock, transforming Fe-Mg-silicates such as olivine, pyroxenes, and amphiboles into serpentine minerals. Gold can be mobilized out of this ultramafic rock via hydrothermal fluids and concentrated as the fluid cools beyond the point which gold is soluble, which it then precipitates out as a solid. This explanation accounts for the source of the gold, the factor mobilizing the gold and the mechanism concentrating the gold. Any gold nuggets found in areas devoid of serpentinized rock could not be formed by this exact mechanism of formation. However in areas without any evidence of serpentinization, it is likely that gold nuggets could still form via fluid-rock interactions, the factor concentrating the nuggets is not the serpentinization, but the fluid interacting with rock. serpentinization and fluid interactions with rocks as a mechanism of formation would exclude any nuggets found with considerable amounts of Os, due to it being considerably less soluble in hydrothermal fluids than the other platinum group elements (Hattori & Cabri, 1992). This exclusion of Os rich nuggets may pose an issue to determining source lithology, as Os isotopic composition is a powerful tool to trace source lithology.

Each of these explanations serve as a good starting point for determining the origin of a gold nugget. Although excluding areas with documented serpentinization and hydrothermal alteration, there currently is not an explanation which relates the processes which concentrate gold into nuggets to the source lithology of which the gold is being concentrated from.

Siderophile Element Fractionation

Differences in element abundances and ratios are instrumental for determining where a rock is sourced. Given that gold is a highly siderophile element and that gold nuggets are primarily composed of gold, the concentrations of highly siderophile elements in the crust and mantle are relevant to this study (Table 1). The upper continental crust has average concentrations of 1.5 ng/g Au, 0.198 ng/g Re, 0.031 ng/g Os, 0.022 ng/g Ir, 0.5 ng/g Pt, 0.34 ng/g Ru, and 0.52 ng/g Pd (Rudnick & Gao, 2004). The primitive mantle has concentrations of 1.49 ng/g Au (Fischer-Godde et al., 2011), 0.28 ng/g Re, 3.4 ng/g Os, 3.2 ng/g Ir, 7.1 ng/g Pt, 5 ng/g Ru, and 3.9 ng/g Pd (McDonough & Sun, 1995). Highly siderophile element concentrations in the primitive mantle are higher than in the continental crust, excluding Au which has subequal concentrations between these reservoirs.

Element	Upper Continental Crust ng/g	Primitive Mantle ng/g
Au	1.5	1.49
Re	0.198	0.28
Os	0.031	3.4
Ir	0.022	3.2
Pt	0.5	7.1
Ru	0.34	5
Pd	0.52	3.9

Table 1: Highly siderophile element concentrations in the upper continental crust and primitive mantle. Upper continental crust average concentrations cited from Rudnick & Gao, 2004, Au concentrations from Fischer-Godde et al., 2011, and other primitive mantle concentrations from McDonough & Sun, 1995.

Osmium and Rhenium as a Proxy

As seen in Table 1 rhenium and osmium abundances are very different in the mantle and crust (Shirey & Walker, 1998). This corresponds to an average $^{187}Re/^{188}Os$ ratio of 0.4 in the mantle, compared to 50 in the crust. Because ^{187}Re decays into ^{187}Os, ^{187}Re has a half-life of 41.6×10^9 years. The ratio between $^{187}Os/^{188}Os$ in a rock can be used as a proxy for provenance, particularly for determining between mafic and ultramafic source rocks. Mafic rocks are broadly crustal in terms of Re and Os, while ultramafic rocks fall closer in line with mantle rocks regarding Re and Os. The average ratio between $^{187}Os/^{188}Os$ in the mantle has been determined to be 0.12737 (Becker et al., 2006). With elevated concentrations of Re in the crust and much lower Os in the crust compared to the mantle, it can be expected that rocks with source lithology from the crust will have a higher $^{187}Os/^{188}Os$ ratio compared to that of the mantle if they are old enough for measurable ingrowth of radiogenic ^{187}Os to occur. The exact amount of enrichment is dependent on the age of the rock and how much Re and Os was in the rock when the rock was deposited on the crust.

Measurable concentrations of osmium (~2 ppb) have been previously found in native gold (Bushmin et al., 2013) suggesting that it may be a viable tracer for the source of the gold. The ratio of $^{187}Os/^{188}Os$ gives context if the gold is sourced from the mantle or the old crust. Although this will only help to deduce the source, and not the process which concentrated the gold. The geologic background of the area, as well as the other trace elements will help to relate nuggets to a specific process of concentration.

Previous Research

A similar study to ours using osmium isotopes in gold was conducted to constrain the source lithology of the gold which was exploited by the people of Mesopotamia and Ur in ancient times (Jansen et al., 2016). This was achieved through analyzing the $^{187}Os/^{188}Os$ ratio, though the samples in this study were processed gold artifacts and not gold nuggets. From their isotopic analysis, the source lithology of the gold artifacts were linked to mantle derived rock, specifically ophiolite complexes near Ur, with the gold artifacts having an average $^{187}Os/^{188}Os$ ratio of 0.128. They also deduced that the gold had to have come from placer deposits. Their reasoning for this was because the Os-Ir inclusions found in the processed gold do not often occur in primary gold deposits, only placers.

In another archaeological study, researchers used $^{187}Os/^{188}Os$ ratios in Celtic gold coins to determine the source lithology of the gold comprising said gold coins. This study found a wide range of ratios including radiogenic values above 0.15, and some values of 0.127, which is the projected mantle ratio. From this they determined their gold must have come from a large layered mafic complex. This would allow for gold from younger rock to maintain a mantle ratio, and older rock to acquire a more radiogenic ratio (Junk& Pernicka, 2003). The age of the rock from which the gold was initially sourced is a key factor in using the $^{187}Os/^{188}Os$ system. Young rock, even if sourced from the crust could produce a non-radiogenic ratio. If this were to be viewed in isolation of the age of the nugget, it could be falsely ascribed as mantle sourced, even if the gold composing the nugget was derived from the crust.

Previous research has also drawn attention to the significance of hydrothermal alteration to Re and Os concentrations within gold sources (Walker et al., 2007). In this study, Os isotopic composition, Re concentration, and platinum group element concentrations were determined for hydrothermally altered gold bearing peridotites, and unmineralized host harzburgites and serpentinites. Osmium isotopic systematics, as well as platinum group element abundances were uniform in the host rocks analyzed. In contrast to the host rocks the hydrothermally altered samples varied in Os isotopic composition and were depleted in Re and PGE. This effect due to hydrothermal alteration could also apply to gold nuggets. Depletion of Re and PGE concentrations could be evidence for hydrothermal alteration, supporting the theory that gold nuggets are formed in hydrothermal systems.

Samples

A set of ten gold nuggets (Figure 1) supplied to the University of Maryland by Fernando Barra, University of Chile were analyzed in this study. The gold nuggets are from placer deposits, 7 of which are collected from rivers on the Osa Peninsula in south eastern Costa Rica, and 3 nuggets were collected from British Columbia.

The 7 Costa Rican gold nuggets were collected from the Agujas, Rincon, Tigre, Carate, and Madrigal Rivers. The British Columbian nuggets were collected from Ruby Creek.

Figure 1: Costa Rican gold nuggets, ruler for scale. Labeled from left to right and top to bottom: Agujas, Adanac C, Adanac B, Adanac A, Rincon, Tigre, Carate C, Carate B, Carate A, Madrigal

Geologic Setting of the Osa Peninsula

The Pacific coast of Costa Rica is characterized by peninsulas and promontories formed by the obduction of ophiolitic segments of oceanic lithosphere, the oldest of which can be dated to the Cretaceous. (Berrange & Thorpe, 1988). One of the peninsulas, the Osa peninsula, is where the nuggets were found. The Osa peninsula is composed of 3 major geologic units: the Nicoya Complex, the Osa Group, and the Puerto Jiménez Group. The Nicoya Complex is composed of basalt-dolerite-gabbro and pelagic sedimentary assemblage, ranging from Senonian to Eocene age (88.5-33.9 Ma). The Osa Group as well as the Puerto Jiménez Group unconformably overlays the Nicoya complex. The Osa Group is composed of semi consolidated greywacke of Pliocene age (5.33-2.5 Ma), and the Puerto Jiménez Group is composed of unconsolidated sediments ranging in age from Pleistocene to Holocene (2.5 Ma-present) (Berrange & Thorpe, 1988).

Economic deposits of gold have been found in both the Osa group, and the Puerto Jiménez Group. These alluvial gold deposits are theorized to have been locally derived from gold-quartz secretion veins present in the underlying Nicoya complex (Berrange & Thorpe, 1988). The geologic map of the Costa Rica is depicted in Figure 2, and the Osa Peninsula in Figure 3, along with rivers associated with the collection of gold nuggets (USGS, 2020).

It is important to note that there are no exposed ultramafic rocks on the Osa Peninsula, though this does not mean that there is no ultramafic material present. Given the fact that the Nicoya Complex is an ophiolite complex, it is highly likely that there are ultramafic rocks somewhere in the rock unit, either undiscovered or potentially unexposed.

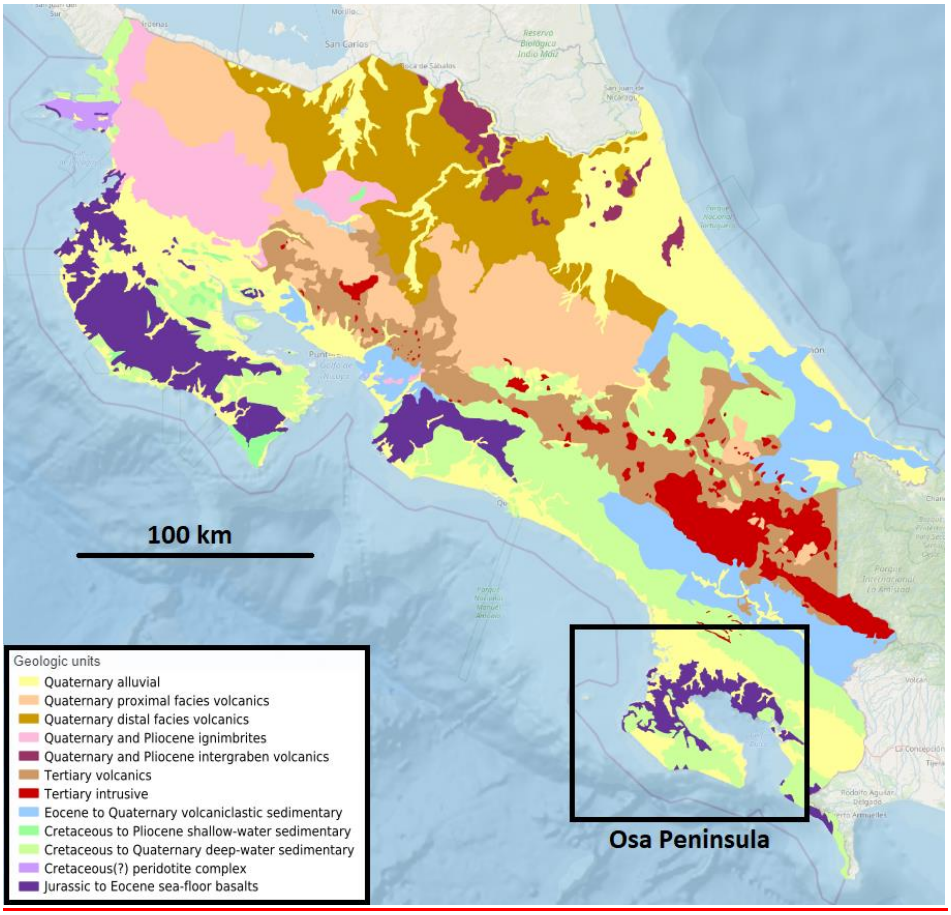

Figure 2: Geologic map of Costa Rica (USGS, 2020).

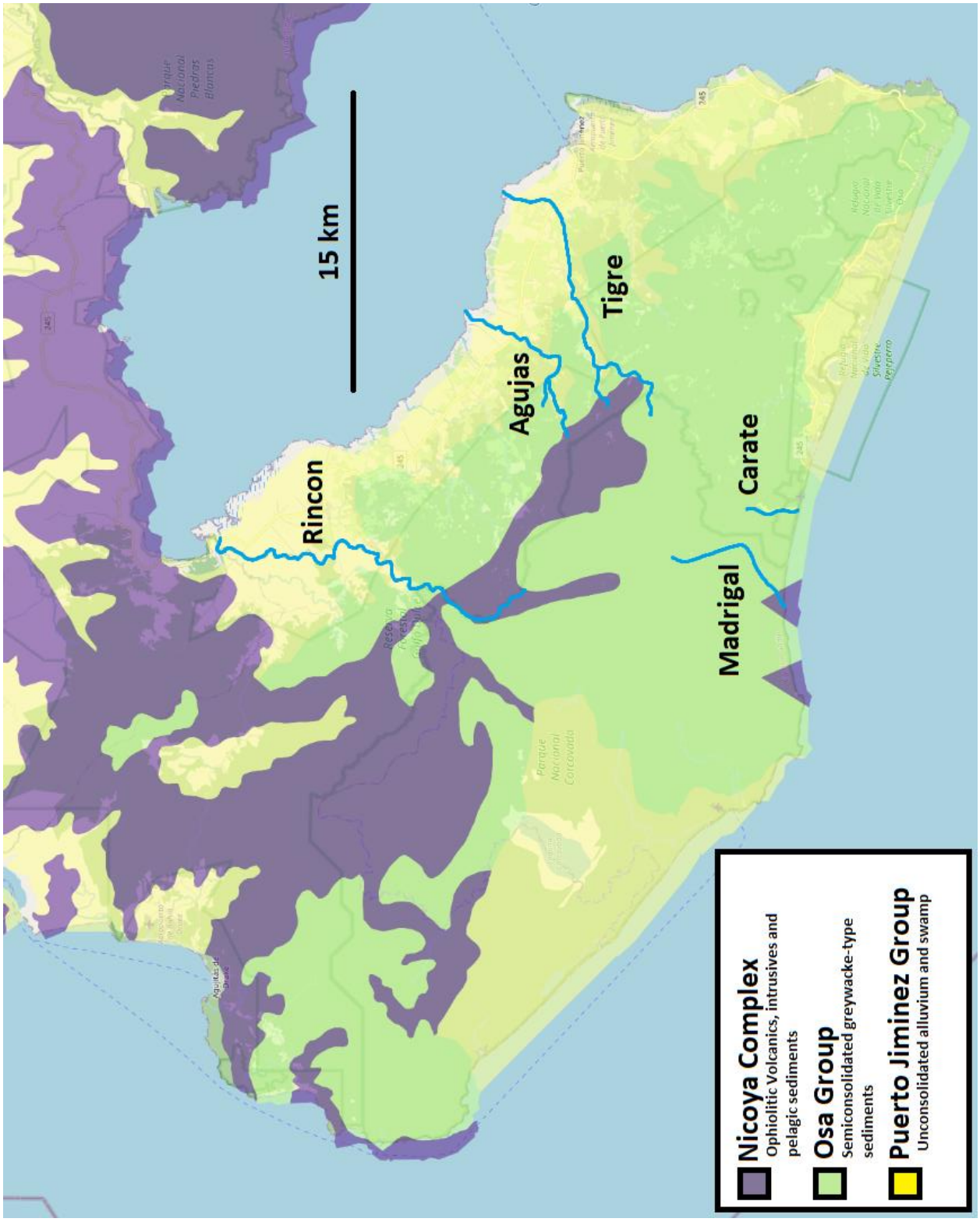

Figure 3: Geologic map of the Osa Peninsula in south eastern Costa Rica (USGS, 2020). Rivers associated with the samples in this study are marked and labeled.

Geologic Setting of the Atlin Area

The placer gold nuggets from British Columbia were collected from Ruby Creek. Ruby Creek flows into Surprise Lake, northeast of the town of Atlin. The Atlin area is characterized by highly deformed and weakly to moderately metamorphosed ophiolitic rocks of the Cache Creek Group, ranging from Pennsylvanian (323.2 Ma – 289.9 Ma) to Permian (298.9 Ma - 47 Ma) in age (Figure 4.). The Cache Creek Group is composed of serpentinites, basalts, limestones, cherts and shales. The strata are cut by two large plutons, the Fourth of July Batholith to the northwest, and by the Surprise Lake Batholith to the northeast. The Fourth of July Batholith is a granodiorite to diorite intrusion of Jurassic (201.3 Ma – 145 Ma) age, while the Surprise Lake Batholith is a granitic to quartz monzonitic intrusion of late-Cretaceous age (100.5 Ma – 66 Ma). The Mount Leonard Stock, a small igneous complex that is located in a north-south oriented strip of the Cache Creek Group cutting through the Surprise Lake Batholith. (Pinsent, 2006)

The Adanac porphyry molybdenum deposit is located near the junction of three major syn to post-mineral faults. The Ruby Mountain fault system runs from northwest to southeast and defines the northeast contact of the molybdenum deposit. This fault system also controls the location of the Ruby mountain volcano, located to the south of the deposit and is relatively young, having likely formed within 10 Ma. An eruption has occurred after the deposition of placer gold bearing gravel in the Ruby Creek drainage. This gravel is covered by both columnar basalt and volcanoclastic debris. The source lithology of the placer gold is uncertain, though it has been theorized to come from both the Surprise Lake Batholith and related intrusions (Pinsent, 2006) and ultramafic precursor material in the Cache Creek Group (Smith, 2009).

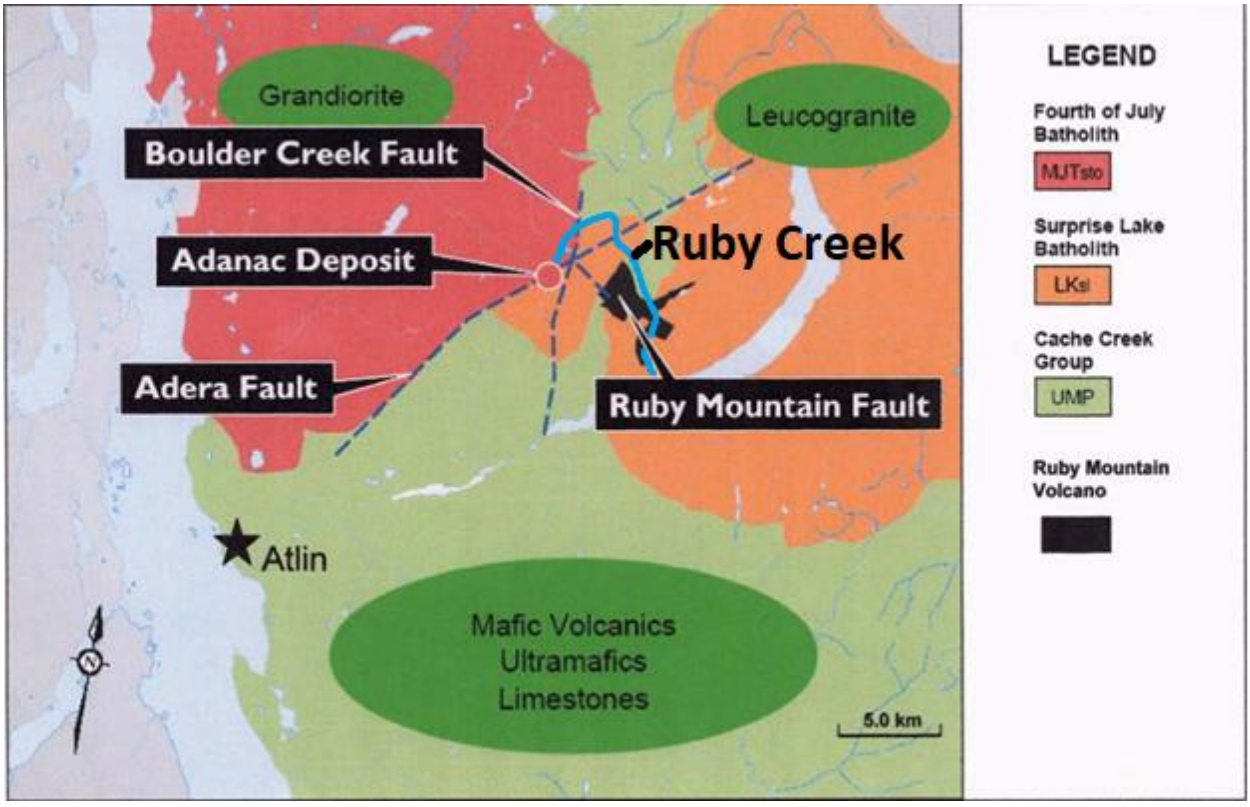

Figure 4: Modified geologic map of the Atlin area (Pinsent, 2006). Ruby Creek has been outlined in blue.

Objectives of Research

The goal of this study is to determine the source lithologies of a set of 10 gold nuggets from placer deposits in both Costa Rica and British Columbia. This was achieved through the determination of siderophile element abundances, and Os isotopic compositions. Of the siderophile elements, Re and Os are of the greatest importance to this study. This is due to the viability of using Os isotopic composition as tracer for the origin of gold. Determination of $^{187}Os/^{188}Os$ within the gold nuggets will be the focus of this study and the primary geochemical tracer used to determine source lithology. The relative abundances of other siderophile elements may provide clues as to the origin of gold when viewed in tandem with the geologic environment of which the nuggets were collected.

Hypothesis I

The gold nuggets will have measurable amounts of Os and Re.

Null Hypothesis I

The gold nuggets will not have measurable amounts of Os and Re.

Hypothesis II

The gold nuggets will have a $^{187}Os/^{188}Os$ ratio consistent with mantle origin.

Null Hypothesis II

The gold nuggets will not have a $^{187}Os/^{188}Os$ ratio consistent with mantle origin.

Methodology

Electron Probe Microanalyzer (EPMA)

To examine the major element composition of the gold nuggets, analyses were completed using an Electron Probe Microanalyzer (EPMA) at the Advanced Imaging and Microscopy Laboratory (AIMLab) at the University of Maryland. The EPMA functions by bombarding the surface of a given sample with a focused electron beam. The electrons in this beam collide with the electron shells of the elements in the sample, forcibly removing some inner shell electrons. This forces electrons from outer shells to release energy in the form of an x-ray, so that it can drop to a lower energy level, and fill the vacancy created by the electron beam. The x-ray released is then used to determine what element released the x-ray. This x-ray released has a characteristic energy and wavelength and can then be quantified to determine concentrations. The electrons from the incident beam are then used to create back-scatter imagery, returning a map of elemental compositions over a given area analyzed by the EPMA. On these back-scatter electron (BSE) images, the brighter regions indicate a higher mean atomic number, and the darker portions indicate a lower mean atomic number. The BSE imagery is primarily used to navigate the sample. A BSE image is depicted in Figure 5.

There are two types of common analyses, energy dispersive spectrometry (EDS) and wavelength dispersive spectrometry (WDS). EDS traditionally is a qualitative analysis technique while WDS is quantitative. In EDS analysis, the energy of x-rays is collected, and the number of x-rays counted and plotted as energy (in keV) versus counts. EDS is generally used as a first order analysis because it returns an approximation of elemental abundances in relation to one another, but not a quantitative concentration of elements. WDS also analyzes the x-ray released by the elements in the sample. Though instead of using the energy of the x-ray, it instead uses the wavelength and angle of refraction of the x-ray to determine concentration more accurately. The x-rays are detected using crystals with specific lattice

spacings placed using Bragg's law [n λ = 2d sinΘ] with n referring to the order of reflection, λ the wavelength of the x-ray, d the spacing between lattice planes and Θ the angle incident angle of the x-ray. Every atom has a characteristic wavelength to its x-rays which it releases when an electron drops to a lower orbital, this is due to every atom having different spacing between each of their orbitals. WDS is more frequently used for quantitative analyses rather than EDS because the wavelength detectors have a better spectral resolution than the EDS detectors., rather than energy released, which in some cases multiple elements release a very similar amount of energy when an electron drops to a lower orbital. EDS in the case of this project, was used more as a tool to navigate around the gold nuggets, and to identify inclusions, whereas WDS was used to collect quantitative analyses.

The EPMA which was used in this project is a JEOL JXA-8900R. It employed an accelerating voltage of 20 kV, a cup current of 50 nA, and a beam diameter of 3 microns. Gold, silver, iron, vanadium, copper, and tungsten were analyzed. We used Kα x-ray lines to detect copper, iron, and vanadium, Lα lines for gold and silver, and Mα lines for tungsten. All x-ray intensities were corrected with a ZAF algorithm.

Normally for WDS analyses, x-ray intensities are measured at both a peak position and multiple background positions. For major elements the counts collected by the EPMA at the peaks are more important than the background counts. Because the data collected is that of major elemental concentrations, Poisson statistics can be used as an effective model to calculate the uncertainty due to counting statistics. The equation used to calculate the uncertainty relative % is: $1\sigma = (1/\sqrt{N}) * 100\%$. In the case of this equation N is the number of counts at the peak position.

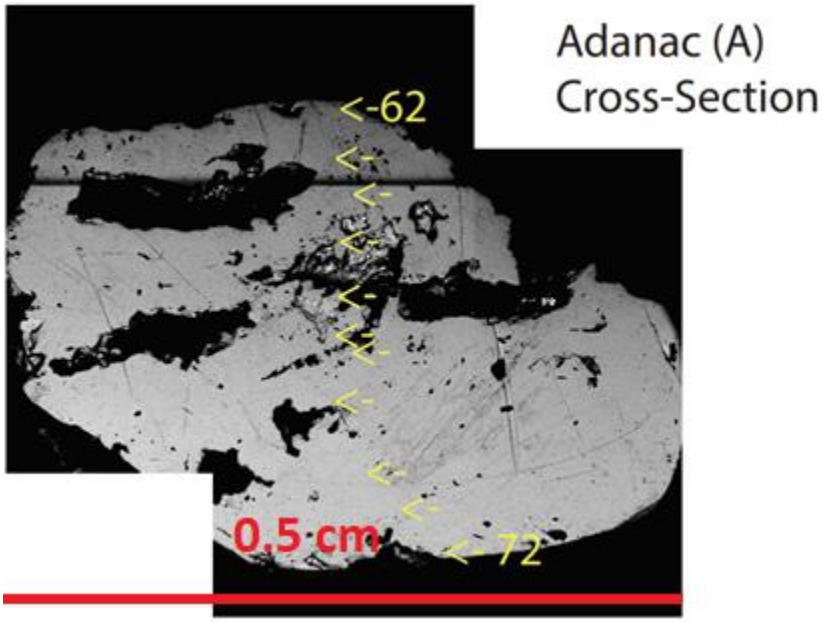

Figure 5: Adanac A. cross-section. Major element composition data were collected at 11 points on the nugget, (indicated by yellow arrows on the figure above, labeled 62 through 72. This data is tabulated on Table 7.

Regarding error in EPMA analyses, accuracy and precision have been assessed and outlined (Table 2, and Table 3). Analyses were conducted on the standards NIST SRM 482 b and a synthetic Pb4Ag6Sb6S16 with the same settings used while analyzing the nuggets. These samples were chosen to evaluate the quality of our Au, Cu and Ag measurements.

Upon analyzing NIST SRM 482 b, the measured values averaged within 1% of the accepted value for Au and Cu, for Ag6Sb6S16, the measured Ag value deviated 2.45% from the accepted value of 23.8%. This is a relatively small % deviation from the accepted values of the standards, meaning that the analyses were accurate, though there is still the factor of human error.

Because the EPMA calculates elemental abundances and concentrations via Bragg's law, the angle which the electron beam hits the surface of a sample effects the accuracy of the measurements. Surface roughness can affect this angle, to mitigate this the nuggets were polished before analysis. While the issue of surface roughness was mitigated, mounting the nuggets still posed a problem. Ideally a sample should be perfectly perpendicular to the instrument during analyses. Given that these gold nuggets were nugget shaped, mounting the surface of the nuggets to be perfectly perpendicular was near impossible. Because of this, the angle which the nuggets were analyzed played a part in the inaccuracy of the EPMA analyses, though the degree of which is difficult to comment on.

NIST SRM 482 b was also used to assess the accuracy of the EPMA analyses. The standard differed in Au content on subsequent analyses, with a coefficient of variation of 0.90%. This is likely due to carbon buildup as the EPMA repeatedly heats the sample during analyses via the electron beam.

Each standard yielded a relatively low % deviation from their known values when analyzed with the same settings used during the analyses of our samples. The EPMA also returned a relatively low coefficient of variation when analyzing Au. The intrinsic error of the EPMA is well within an acceptable range to view any analyses done on our samples with it as quantitative.

EPMA: Determination of Accuracy			
Standard:	**NIST SRM 482 b**		**Pb4Ag6Sb6S16**
# of analyses	**Au**	**Cu**	**Ag**
1	80.07	20.05	23.31
2	80.19	20.13	22.72
3	80.29	20.20	23.18
4	79.26	20.01	23.46
5	80.02	19.71	23.39
Average of analyses on EPMA	**79.96**	**20.02**	**23.22**
Std Deviation	**0.41**	**0.19**	**0.29**
Accepted Value of Standard	**80.15**	**19.83**	**23.8**
% Dev from Accepted Value	**0.23%**	**-0.94%**	**2.45%**

Table 2: Determination of Accuracy for EPMA analyses. The standards NIST SRM 482 b and Pb4Ag6Sb6S16 were analyzed 5 times each with the same settings used while analyzing the nuggets. NIST SRM 482 b was analyzed to assess the accuracy of Au and Cu measurements, while Pb4Ag6Sb6S16 was used to assess the accuracy of Ag measurements. NIST SRM 482 b is a silver copper alloy with an accepted composition of 80.15% Au and 19.83% Cu, Pb4Ag6Sb6S16 is a synthetic lead silver antimony sulfide with an accepted Ag composition of 23.8%.

EPMA: Estimate of Precision of Au Analysis	
Standard	NIST SRM 482 b
# of analyses	Au
1	79.48
2	79.76
3	79.49
4	80.16
5	78.25
Average	79.43
Std Deviation	**0.713**
CV	**0.90%**

Table 3: Estimate of precision of Au analyses via EPMA. NIST SRM 482 b was analyzed 5 times to assess the precision of Au analyses via EPMA. These 5 measurements were averaged together, and their standard deviation as well as coefficient of variation were calculated.

Laser Ablation Inductively Coupled Plasma Mass Spectrometry (LA-ICP-MS)

To determine the trace element abundances of the gold nuggets, analyses were completed using an Element 2 Inductively Coupled Plasma Mass Spectrometer, coupled to a New Wave UP213 laser ablation system. The LA-ICP-MS functions by ablating the surface of a given sample with a focused laser beam. The particles are ablated into a stream of helium gas which is then mixed with argon gas and introduced into an argon plasma. The plasma results in the atomization and ionization of the particles. After ionization, the ions are accelerated into the mass spectrometer and pass through a field which diverts ions according to their mass-charge ratio. Isotopes of a selected element, chosen to avoid potential interferences, are then directed through an electric field and onto a detector for measurement. The isotopes analyzed in this study were (^{31}P, ^{51}V, ^{53}Cr, ^{57}Fe, ^{59}Co, ^{61}Ni, ^{63}Cu, ^{71}Ga, ^{74}Ge, ^{75}As, ^{95}Mo, ^{97}Mo, ^{101}Ru, ^{103}Rh, ^{105}Pd, ^{107}Ag, ^{183}W, ^{185}Re, ^{189}Os, ^{193}Ir, ^{195}Pt).

The LA-ICP-MS is most accurate when performing an analysis on a single spot, but can be rastered over a larger area to find differences in composition across an area. Examples of the surface being ablated in both line analysis and spot analysis are depicted on the sample Agujas in Figure 6. It was noted in Jansen et al. (2016) that some gold contained microscopic inclusions of platinum group element nuggets. To determine if any of our nuggets had any such inclusions, we performed a line analysis with the LA-ICP-MS.

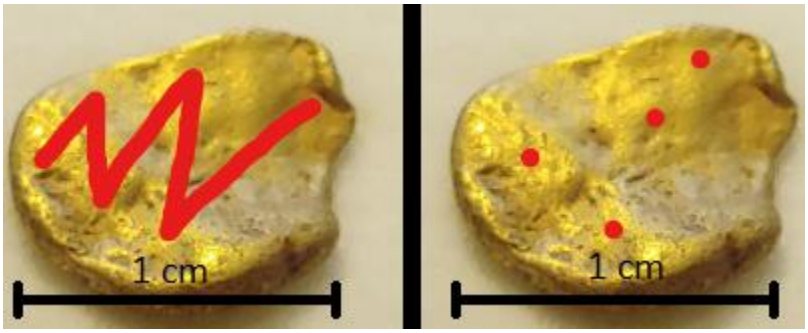

Figure 6: Example of a line analysis (left) and spot analysis (right)

The LA-ICP-MS concentrations are determined by comparing the measured isotopes in a standard with those of the sample. This requires an element of known concentration in the standard and in the sample. Ideally the composition of the standard and sample would be the same to avoid elemental fractionation due to matrix effects. This raised an interesting dilemma in our analyses, given the fact that we did not have a "gold standard" to compare our nuggets to. To remedy this, we used the iron meteorite Coahuila, as a standard which has trace concentrations of gold and other HSE. In the initial analyses we had no elements in common between the iron meteorite and the nuggets. Gold could not be analyzed as the concentration was too high to measure. Initial attempts using the known concentration of Ir in Coahuila, and estimating the Ir content of the nuggets from the counts failed when it was realized that the gold was not resolved from the Ir in the mass spectrometer. In the end Cu was used as the internal standard element, using the mean Cu concentration from the electron probe as an input. The TIMS employed in this study can accurately measure picograms of Os. The intrinsic error of the Os measurements is +/- 0.2%.

Isotope Dilution

To examine the ratio of $^{187}Os/^{188}Os$ in the bulk samples of the gold nuggets as well as the elemental abundances of Re, Ir, Ru, and Pd in bulk nuggets, the nuggets were first dissolved in a mixture of HNO_3, HCl, along with appropriate quantities of ^{190}Os, ^{185}Re, ^{191}Ir, ^{99}Ru, ^{194}Pt and ^{105}Pd spikes. These mixtures were then sealed in a chilled 25 mL borosilicate Carius Tubes (CTs). These CTs were then be heated to 270°C for 24 hours. A CCl_4 solvent was then used to extract osmium from the acid solution then further back-extracted into HBr, and finally purified through microdistillation.

Re, Ir, Pt, Ru, and Pd which were not extracted by the CCl_4 solvent were first dried and redissolved into 2.5 ml HCl, then purified via anion exchange columns. The columns were first filled with anion exchange resin, then sequentially washed with 5 ml H_2O, 3 ml 0.8 M HNO_3, 2 rounds of 10ml concentrated quartz distilled HNO_3, 3 ml of 0.8 M HNO_3, 2 ml of H_2O, 2 ml of 1 M HCl, 10 ml of concentrated quartz distilled HCl, and 2 rounds of 2 ml of 1 M HCl. Then the dissolved samples were loaded onto the columns and eluted with 2 rounds of 6 ml of 1M HCl + 1M HF. The Re and Ru cut of the columns were collected by then passing 12 ml of 6M HNO_3 through the columns, Pt and Ir were collected by passing 12 ml of concentrated HNO_3 through the columns. The columns were then rinsed with 2 ml H_2O and the remaining Pd cut was collected by passing 12 ml of concentrated quartz distilled HCl through the columns. Due to the similar atomic weight of Au, Ir, and Pt, high concentrations of Au can interfere with any measurements of these two elements. This is normally never an issue, given that gold is generally a trace element. In the case of these nuggets, the gold concentrations are sufficiently high that it can pose an issue in collecting accurate Ir and especially Pt data. Because of this, the Ir and Pt cuts of the nuggets could not be measured, and as a workaround Ir and Pt concentrations in the Re and Ru cuts of the nuggets were measured instead. The Pd cuts of the nuggets were dried down after being collected and reprocessed through the columns in order to reduce the amount of gold present in the Pd cuts. Whenever an element is measured on the ICP-MS, it leaves behind a background signal of that given element on future tests. This is also usually never an issue with gold, given that it is generally a trace element when measured. A high concentration of gold can lead to a high gold background signal on the ICP-MS for subsequent tests, making trace gold unmeasurable on the given instrument. To help mitigate this, the Pd cuts of the nuggets were run through the columns a second time to purge some of the remaining gold in that cut. The 3 cuts for each nugget were then dried and each dissolved in 5% nitric acid to be analyzed via solution ICP-MS.

Thermal Ionization Mass Spectroscopy (TIMS)

After the osmium was extracted, negative thermal ionization mass spectrometry (N-TIMS) was employed to analyze the isotopic ratios of $^{187}Os/^{188}Os$. The samples were analyzed via the Triton mass spectrometer. The mass spectrometer functions by first ionizing the sample by heating a filament and concentrating an ion beam into a flight. The ion beam is the redirected with an electromagnet into a secondary electron multiplier (SEM) as the detector. The SEM works by multiplying an incident charge. This process is called secondary emission in which a single electron induces the emission of multiple electrons when bombarded on a secondary emissive material. This process is repeated on multiple layers of metal plates with an electric potential applied between these plates. This repetition results in a shower of electrons collected by a metal anode which are then used as a proxy for counts. In this case we were looking for ^{187}Os and ^{188}Os. The uncertainties of Os concentrations and isotopic compositions is +/- 0.2%.

Solution Inductively Coupled Plasma Mass Spectrometry

Re, Ir, Ru, Pt, and Pd were analyzed via Solution ICP-MS. This was conducted on the Element 2 similarly to the LA-ICP-MS analyses. The only difference in processing is that the material being analyzed is aerosolized after being dissolved in a solution, rather than being ablated from a solid surface. This is a much more accurate method to assess the relative abundances of a given element than LA-ICP-MS, primarily due to the isotope dilution perform beforehand. The isotope dilution isolates the desired elements yielding a much higher concentration of these elements than if they were to be analyzed on a bulk sample without first being purified. The solution ICP-MS compares elements to that of known standards similarly to LA-ICP-MS. Solutions were prepared of 200 ppt Re, 200 ppt Pd, 200 ppt Pt, 500 ppt Ru, 5 ppb Pd, 5 ppb Ru, 200 ppt Ir standards, and a 100ppb Pt 50ppb Ir standard to calibrate the mass spectrometer. The uncertainties of these measurements were +/- 5%.

Results

To gather baseline information on the nuggets and to determine how further research would be approached, preliminary measurements were collected. Among these measurements, the gold nuggets were weighed, accessory phases were identified, and qualitative trace siderophile element compositions were determined. Platinum data here was not collected due to difficulties regarding Au interference with ICP-MS measurements.

The measured weight of each respective gold nugget, as well as the observed phases other than gold present on the surface of the nuggets, has been determined (Table 4). The mineralogy on the surfaces of the nuggets is not guaranteed to be representative of the environment in which the nuggets formed, these phases could have been placed during the nuggets travel along the streambed. The phases were determined via EPMA analyses.

Sample	Weight (mg)	Observed Phases on Surface
Agujas	1627.63	Calcite, Iron-oxides, Iron-oxide-hydroxides
Adanac A	406.94	Quartz, Amphibole
Adanac B	337.98	Calcite
Adanac C	171.83	Chlorite
Tigre	555.48	Iron-oxides, Iron-oxide-hydroxides, Chlorite
Rincon	593.23	Chlorite
Carate A	190.77	Chlorite, Epidote, Amphibole
Carate B	225.05	Iron-oxide, Epidote, Amphibole
Carate C	190.81	Quartz, Chlorite
Madrigal	675.92	Quartz, Amphibole

Table 4: Measured weights of each sample and observed phases on the surface of each nugget.

Trace siderophile element concentrations of all 10 nuggets were first determined via LA-ICP-MS line analyses (Table 5). Line analyses were used to assess the homogeneity of the trace elements distributed throughout the nugget. The nuggets were found to be mostly homogenous on the surface. Notably the Adanac nuggets are highly enriched on the surface with Re and Os compared to the other samples. The nuggets also all have much higher concentrations of Os compared to Re. The line analysis data is qualitative at best due to Au interference yielding potentially compromised Ir data, and that the standards used were a poor fit for the samples analyzed.

After line analyses were conducted, the nuggets trace element concentrations were then determined via spot analysis (Table 6). The spot analyses were primarily conducted to determine how much spike was needed in our first round of the isotope dilution process. Spot analyses were chosen over line analyses to determine spike weights because spot analyses are generally more accurate than line analyses. Notably, the spot analyses returned a much lower concentration of Re and Os compared to the line analyses (Table 5). All ten samples were determined to still have much higher concentrations of Os than Re, much like the line analyses. It is important to note that without a proper gold standard, this data is likely to have a very large relative error (>10%) compared to the actual concentrations of trace elements.

LA-ICP-MS Line Analysis Concentrations						
		Agujas	Adanac (a)	Adanac (b)	Adanac (c)	Rincon
%	P	b.d.	b.d.	b.d.	b.d.	0.00076
mg/g	V	0.12	b.d.	0.020	b.d.	b.d.
µg/g	Cr	b.d.	b.d.	b.d.	b.d.	b.d.
mg/g	Fe	0.081	b.d.	b.d.	0.15	0.0013
µg/g	Co	b.d.	b.d.	0.45	b.d.	0.033
µg/g	Ni	0.77	b.d.	1.4	2.9	b.d.
µg/g	Cu	1100	900	3200	6000	500
µg/g	Ga	0.036	0.24	0.12	0.70	0.005
µg/g	Ge	b.d.	b.d.	b.d.	b.d.	b.d.
µg/g	As	b.d.	b.d.	0.084	0.28	0.022
µg/g	Mo	0.003	b.d.	0.037	0.12	0.01
µg/g	Ru	0.005	0.62	0.027	0.028	0.001
µg/g	Rh	0.045	1.1	0.16	0.41	0.019
µg/g	Pd	1.0	560	25	160	1.3
µg/g	W	0.003	0.30	0.19	8.6	0.004
µg/g	Ir	0.60	31	2.2	12	0.97
ng/g	Re	b.d.	b.d.	b.d.	b.d.	b.d.
ng/g	Os	11	390	18	200	6
		Tigre	Carate (a)	Carate (b)	Carate (c)	Madrigal
%	P	0.0027	b.d.	0.011	b.d.	b.d.
mg/g	V	0.56	b.d.	b.d.	0.012	0.41
µg/g	Cr	0.21	0.28	6.0	b.d.	12
mg/g	Fe	0.012	0.0016	2.8	0.0076	0.050
µg/g	Co	0.26	0.12	1.9	b.d.	9.2
µg/g	Ni	b.d.	0.10	b.d.	b.d.	b.d.
µg/g	Cu	700	100	100	400	5000
µg/g	Ga	0.35	0.043	2.0	0.029	0.93
µg/g	Ge	b.d.	b.d.	b.d.	0.023	b.d.
µg/g	As	0.30	b.d.	0.29	b.d.	b.d.
µg/g	Mo	0.97	0.002	28	0.001	0.13
µg/g	Ru	0.003	b.d.	0.002	0.001	0.13
µg/g	Rh	0.039	0.004	0.004	0.011	0.18
µg/g	Pd	1.1	0.18	0.38	0.27	2.8
µg/g	W	0.013	0.006	0.030	0.006	0.058
µg/g	Ir	0.41	0.040	0.36	0.16	6.8
ng/g	Re	b.d.	b.d.	91	b.d.	b.d.
ng/g	Os	3	b.d.	1	2	60

Table 5: Averaged Trace siderophile element concentrations determined via line analyses. The detection limit of the LA-ICP-MS set for this study is 1 ng/g, any value below this has been marked as bd. Copper concentrations from electron probe data were used as an internal standard to calculate concentrations in this table. Silver data has been omitted because it was saturated and therefore inaccurate.

LA-ICP-MS Spot Analysis Concentrations						
		Agujas	Adanac (a)	Adanac (b)	Adanac (c)	Rincon
%	P	0.040	0.028	0.007	0.002	0.001
%	Ag	3.4	24	26	23	5.2
mg/g	V	10	25	1.8	2.7	1.4
µg/g	Cr	2.9	31	17	7.4	8.6
mg/g	Fe	11	110	10	7.7	1.3
µg/g	Co	3.8	64	16	26	2.1
µg/g	Ni	18	390	56	130	17
µg/g	Cu	2900	320	130	36	670
µg/g	Ga	1.7	11	3.7	3.6	0.33
µg/g	Ge	2.4	1.0	0.75	0.58	0.21
µg/g	As	4.9	73	16	11	b.d.
µg/g	Mo	0.66	35	2.3	1.5	0.26
µg/g	Ru	0.01	0.05	0.02	0.03	b.d.
µg/g	Rh	0.15	0.03	0.02	0.01	0.04
µg/g	Pd	0.55	0.74	0.39	0.13	0.24
µg/g	W	6.9	8800	4900	2700	6.6
µg/g	Ir	0.37	0.74	0.39	0.27	0.32
ng/g	Re	1	1	5	10	4
ng/g	Os	30	90	10	20	10
		Tigre	Carate (a)	Carate (b)	Carate (c)	Madrigal
%	P	0.0002	0.010	0.002	0.007	0.008
%	Ag	13	1.8	4.7	4.3	6.0
mg/g	V	1.6	8.2	8.4	4.7	14
µg/g	Cr	1.3	4.6	1.7	11	6.7
mg/g	Fe	0.8	5.7	1.8	33	7.8
µg/g	Co	1.70	2.8	2.7	5.6	12
µg/g	Ni	12	18	1.6	45	50
µg/g	Cu	940	57	1300	1100	1700
µg/g	Ga	0.49	1.7	0.29	4.4	2.3
µg/g	Ge	b.d.	0.45	0.49	1.8	0.56
µg/g	As	0.72	0.84	1.2	1.5	4.3
µg/g	Mo	0.07	0.25	6.0	0.05	4.2
µg/g	Ru	b.d.	0.01	b.d.	0.02	0.005
µg/g	Rh	0.04	0.002	0.11	0.06	0.08
µg/g	Pd	0.35	0.24	0.25	0.27	0.48
µg/g	W	b.d.	b.d.	4.2	7.5	4.0
µg/g	Ir	0.23	0.43	0.35	0.28	0.41
ng/g	Re	2	1	0	3	4
ng/g	Os	30	30	3	9	70

Table 6: Siderophile element concentrations of gold nuggets determined via spot analyses. As with previous tables, b.d. is indicative of a measurement being below detection. Silver concentrations from electron probe data were used as an internal standard to calculate concentrations in this table.

The difference in siderophile element concentrations between the line analyses and spot analyses is indicative of the nuggets having some elements concentrated in a surface layer (Table 5 & Table 6). The exact mechanisms which would concentrate siderophile elements into a micron thick layer on the surface of the nuggets is unknown, but may relate to the residence in the streambed. Analyzing the leachate separately from the nugget may give clues as to how the surface concentration occurred and if it has any bearing on the formation of the nuggets.

Adanac (a) was analyzed alone to first test how the gold nuggets would behave on the instruments. This was also done to determine how impactful the surface enrichment of certain siderophile elements would be on the measurements of the bulk samples. To avoid the enrichment of siderophile elements on the surface of the nuggets, and to measure the interior concentrations of siderophile elements in Adanac (a), the nugget was cut in half to create a fresh surface. The interior was then polished to remove any residue from the exterior of the nugget.

Major element compositions of the polished cross section of Adanac (a) were determined via EPMA (Table 7) with uncertainties presented in relative percent (Table 8). Adanac (a) was measured to be 24.27% silver by weight percent, high enough to be considered electrum (gold containing at least 20% silver). To determine if the nugget had any zoning of major elements, multiple locations were probed on the interior of the nugget. Adanac (a) was determined to be mostly homogenous, with similar concentrations of major elements throughout the interior. These analyses were the first quantitative values of the study, given its relatively low error (Table 8) and therefore the Ag and Cu concentrations found via EPMA were used as the internal standard for the LA-ICP-MS analysis. Importantly, these known values helped to reduce error in the spot analyses which were then used as guidelines for spiking during isotope dilution.

EPMA Adanac (a) Interior Major Element Composition (Weight %)					
Traverse #	**Au**	**Fe**	**Ag**	**Cu**	**Total**
62	72.11	b.d.	25.97	0.04	98.11
63	67.02	b.d.	24.13	0.01	91.16
64	72.21	b.d.	25.06	0.01	97.28
65	68.96	b.d.	24.47	0.01	93.45
66	73.00	b.d.	24.74	0.44	98.18
67	72.58	b.d.	24.39	b.d.	96.96
68	71.98	b.d.	24.10	b.d.	96.08
69	72.44	b.d.	23.92	b.d.	96.36
70	73.03	0.01	23.55	b.d.	96.59
71	71.51	0.02	22.36	b.d.	93.88
Mean	**71.48**	**0.01**	**24.27**	**0.10**	**95.81**

Table 7: Major element composition of the polished cross section of Adanac (a) The traverse numbers in the leftmost column correspond to the yellow arrows depicted in figure 4. V and W were also attempted to be measured, both of which were below detection. Any concentrations lower than 0.001 weight % are below the detection threshold. This has been indicated with b.d. on the table.

EPMA Adanac (a) Interior Major Element Composition Uncertainty Relative % (1σ)				
Traverse #	**Au**	**Fe**	**Ag**	**Cu**
62	0.63	N/A	0.33	34.79
63	0.65	N/A	0.35	>100
64	0.63	N/A	0.34	>100
65	0.66	N/A	0.34	96
66	0.63	N/A	0.34	3.2
67	0.64	N/A	0.35	N/A
68	0.64	N/A	0.35	N/A
69	0.64	N/A	0.35	N/A
70	0.64	98	0.35	N/A
71	0.64	55	0.36	N/A

Table 8: Error in relative percent of major element composition of Adanac (a)'s polished cross section

The trace siderophile element concentrations of the polished interior of Adanac (a) were determined (Table 9). Notably, the siderophile element concentrations found on the interior of Adanac (a) were higher than those found during spot analyses but lower than those found during line analyses. The Re concentration was also determined to be orders of magnitude lower than the Os concentrations in these analyses, much like the spot and line analyses.

LA-ICP-MS Adanac (a) Interior Siderophile Element Concentrations			
		Adanac (a) Interior	rsd (%)
µg/g	V	2.3	137
µg/g	Cr	41	621
µg/g	Co	0.75	478
µg/g	Ni	30	627
mg/g	Cu	0.20	1320
µg/g	Ga	0.37	89.2
µg/g	Ge	0.32	97.0
µg/g	As	0.62	103
µg/g	Se	0.80	535
ng/g	Ru	10	1075
µg/g	Rh	0.12	563
µg/g	Pd	3.1	65
µg/g	Sb	24	93
µg/g	W	0.49	1480
ng/g	Re	6.1	909
µg/g	Os	0.10	330
µg/g	Ir	0.69	104

Table 9: Siderophile element concentrations of the polished interior of Adanac (a). Because of the high relative standard deviation, these concentrations were used qualitatively as guidelines for spiking the nuggets.

Os concentration and the $^{187}Os/^{188}Os$ ratio of Adanac (a) were determined via TIMS (Table 10). The leachate and nugget yielded different $^{187}Os/^{188}Os$ ratios, though both ratios are similar to that of the mantle.

TIMS Adanac (a) Osmium Isotopic Composition			
	Os (pg)	Os (ng/g)	$^{187}Os/^{188}Os$
TABs	1.4	N/A	0.129 ± 0.002
Leachate	18.98	33.00	0.1277 ± 0.0013
Leached Nugget	51.03	0.497	0.1315 ± 0.0013

Table 10: TIMS osmium isotopic analysis of Adanac (a). Two total analytical blanks (TAB) were measured, 2.0 and 0.8 picograms, with 0.1270 and 0.1312 $^{187}Os/^{188}Os$ ratios respectively. These were averaged together to obtain an average blank of 1.4 ± 0.6 pg, and a $^{187}Os/^{188}Os$ ratio of 0.129 ± 0.002, as displayed in the table.

Quantitative highly siderophile element concentrations for Adanac (a) were collected via solution ICP-MS (Table 11). Due to a difference in surface and interior concentrations illustrated in previous tables, the nugget was leached of approximately 1% of its weight. Each cuts of the nugget were then analyzed separately. The Re cut for the leachate was contaminated during analyses and is therefore not reported. Notably the leachate and interior follow a similar trend to previous analyses, with the leachate being enriched in highly siderophile elements compared to the interior. Ir and Pt were notably difficult to analyze via solution ICP-MS due to interference from the high concentrations of Au in the dissolved Ir and Pt fractions of the nugget.

Adanac (a) Isotope Dilution Siderophile Element Concentrations (ppb)		
Element	**Leachate**	**Nugget**
Os	33.0	0.50
Re	N.D.	0.17
Pd	120	b.d.
Ru	b.d.	b.d.
Ir	5.83	0.11

Table 11:Isotope dilution siderophile element concentrations collected via solution ICP-MS for Adanac (a). The Re cut for the leachate was contaminated during analyses and is therefore not reported.

After analyzing Adanac (a) and learning how gold nuggets behave on anion exchange columns as well as during TIMS, solution ICP-MS, and LA-ICP-MS analyses, the remaining nuggets were analyzed in bulk. It was determined that the surface concentration, while higher than the interior of the nugget, was not high enough to affect the concentration of the bulk sample significantly, given that it only composed 1% of the nuggets weight. Because of this, the remaining nuggets were not leached before analysis. Adanac (a) was also analyzed again for consistency between the samples.

Major element composition of the polished cross sections of each of the other 9 nuggets were determined via EPMA and tabulated along with the EPMA measurements of Adanac (a) (Table 12). All of the nuggets were homogenous, with relatively low standard deviation of elemental abundances throughout the nuggets. Like with Adanac (a), the EPMA analyses were conducted to use the more accurate ELMA measured elemental concentrations as an internal standard to reduce error in the LA-ICP-MS analyses.

EPMA Major Element Concentrations						
		Agujas	**Adanac (a)**	**Adanac (b)**	**Adanac (c)**	**Rincon**
Au	**Wt. %**	**95.50**	**71.21**	**81.26**	**77.61**	**97.96**
	Stdev.	1.92	2.06	2.50	2.60	2.59
Fe	**Wt. %**	**0.00**	**0.01**	**0.00**	**0.03**	**0.02**
	Stdev.	0.02	0.01	0.02	0.03	0.01
Ag	**Wt. %**	**2.69**	**23.02**	**17.39**	**19.85**	**1.90**
	Stdev.	0.18	4.22	0.43	1.25	0.48
Cu	**Wt. %**	**0.11**	**0.09**	**0.32**	**0.60**	**0.05**
	Stdev.	0.03	0.17	0.12	0.37	0.02
Total Wt. %		**98.30**	**94.29**	**98.96**	**98.09**	**99.93**
		Tigre	**Carate (a)**	**Carate (b)**	**Carate (c)**	**Madrigal**
Au	**Wt. %**	**99.26**	**94.49**	**102.72**	**100.29**	**95.65**
	Stdev.	4.19	4.88	3.24	2.44	2.31
Fe	**Wt. %**	**0.03**	**0.01**	**0.15**	**0.00**	**0.00**
	Stdev.	0.04	0.02	0.08	0.01	0.01
Ag	**Wt. %**	**2.43**	**4.56**	**0.19**	**0.80**	**4.09**
	Stdev.	1.37	2.44	0.05	0.53	0.14
Cu	**Wt. %**	**0.07**	**0.00**	**0.00**	**0.04**	**0.50**
	Stdev.	0.03	0.03	0.03	0.05	0.09
Total Wt. %		**101.79**	**99.05**	**103.04**	**101.12**	**100.23**

Table 12: Major element composition of the polished cross sections of each nugget. Standard deviation is included to assess the homogeneity of the interior of the nuggets, all of which were homogenous with no indication of zoning in the polished cross section.

The trace siderophile element concentrations of the polished interior of each nugget were determined (Table 13). The nuggets were sawed in half, polished, then their polished cross sections were analyzed via LA-ICP-MS spot analyses. This was done to avoid the concentration of siderophile elements on the surface of the nuggets and to return a measurement more accurate to the bulk sample. Like with Adanac (a), this was used to establish the amount of spike needed to be used during isotope dilution. The siderophile element concentrations found on the interiors were higher than those found during spot analyses (Table 4) but lower than those found during line analyses (Table 5). The Re concentration was also determined to be lower than the Os concentrations in these analyses.

LA-ICP-MS Interior Concentrations (µg/g)						
		Agujas	Adanac (a)	Adanac (b)	Adanac (c)	Rincon
%	P	b.d.	b.d.	b.d.	b.d.	0.17
µg/g	V	b.d.	b.d.	b.d.	b.d.	b.d.
µg/g	Cr	b.d.	b.d.	b.d.	b.d.	13
µg/g	Fe	570	b.d.	b.d.	410	730
µg/g	Co	b.d.	b.d.	10	b.d.	5.2
µg/g	Ni	14	b.d.	32	11	b.d.
µg/g	Cu	8600	95.0	9600	4500	8700
µg/g	Ga	0.21	0.02	0.3	0.1	0.4
µg/g	Ge	b.d.	b.d.	b.d.	b.d.	b.d.
µg/g	As	b.d.	b.d.	2.0	0.11	3.8
µg/g	Mo	0.09	0.10	0.06	0.07	10
µg/g	Ru	0.38	0.13	0.53	0.23	0.60
µg/g	Rh	0.36	0.12	0.50	0.23	0.58
µg/g	Pd	1.6	6.6	5.1	6.0	2.7
µg/g	W	0.02	0.05	0.47	1.5	0.20
µg/g	Re	b.d.	b.d.	b.d.	b.d.	0.03
µg/g	Os	0.08	0.04	0.02	0.08	0.04
µg/g	Ir	4.5	3.2	3.1	3.8	4.3
µg/g	Pt	86	61	61	68	80
		Tigre	Carate (a)	Carate (b)	Carate (c)	Madrigal
%	P	0.11	b.d.	0.15	b.d.	b.d.
µg/g	V	b.d.	b.d.	b.d.	500	340
µg/g	Cr	b.d.	88	45	b.d.	42
µg/g	Fe	180	490	28000	610	170
µg/g	Co	4.9	19	14	b.d.	32
µg/g	Ni	b.d.	31	b.d.	b.d.	b.d.
µg/g	Cu	10000	8600	3300	12000	3700
µg/g	Ga	0.11	0.6	8	1.4	0.7
µg/g	Ge	b.d.	b.d.	b.d.	1.4	b.d.
µg/g	As	3.2	b.d.	2.6	b.d.	b.d.
µg/g	Mo	0.87	0.02	140	0.06	0.08
µg/g	Ru	0.51	0.33	0.16	0.37	0.13
µg/g	Rh	0.46	0.33	0.14	0.34	0.13
µg/g	Pd	2.0	2.8	1.2	1.8	1.7
µg/g	W	0.15	0.56	0.25	0.14	0.05
µg/g	Re	0.00	0.05	1.2	b.d.	b.d.
µg/g	Os	0.01	0.01	0.02	0.05	0.04
µg/g	Ir	4.7	3.3	3.4	4.3	3.9
µg/g	Pt	84	60	64	79	70

Table 13: Siderophile element concentrations of the polished interior of each nugget. The relative standard deviation for each element ranges greatly. This is due to the relatively low abundances of measured elements. Because of the high relative standard deviation, these concentrations were primarily used as guidelines for spiking the nuggets during isotope dilution.

Highly siderophile element concentrations for each nugget were collected via solution ICP-MS (Table 14). Osmium and Re concentrations vary in ratio from nugget to nugget. While attempted precautions were taken to avoid Au interference with Ir and Pt measurements, inevitably sufficient Au concentrations remained in solution with the Ir and Pt fractions to interfere with any Pt measurements to be taken from many of the nuggets. The Au concentration was low enough to not interfere with Ir measurements in all analyses. Rhenium for Carate (b) was under spiked, because of this the value is not reported. Iridium data for Adanac (a) was not reported due to Au interference.

Bulk Isotope Dilution Siderophile Element Concentrations (ppb)					
Element	**Madrigal**	**Carate (c)**	**Carate (b)**	**Carate (a)**	**Rincon**
Os	1.19	1.63	1.07	0.985	0.137
Re	1.03	0.598	N.D.	0.406	9.63
Pd	8.68	72.5	12.1	10.8	772
Ru	0.630	0.916	0.624	0.635	0.096
Ir	1.34	2.15	1.23	1.60	0.290
Element	**Tigre**	**Adanac (c)**	**Adanac (b)**	**Adanac (a)**	**Agujas**
Os	0.031	1.32	0.637	0.857	5.79
Re	3.15	2.15	6.36	3.77	1.06
Pd	10.3	18.3	58.5	6.2	47.0
Ru	0.046	0.695	0.205	0.304	0.865
Ir	0.229	14.4	0.613	N.D.	5.15

Table 14: Highly siderophile element concentrations of all 10 nuggets listed in ppb. N.D. denotes a missing value, either due to Au interference or over/under spiking.

Osmium concentration and the $^{187}Os/^{188}Os$ ratio of the nuggets were determined via TIMS (Table 15). Madrigal, Carate (c), Carate (a), Adanac (c), Adanac (b), and Agujas all yielded $^{187}Os/^{188}Os$ ratios like that of the mantle, while Rincon and Tigre have a comparatively more radiogenic ratio. Rincon and Tigre have a higher $^{187}Re/^{188}Os$ than the other nuggets. The model ages listed in the table are based upon the assumption that the precursor material which the nuggets are derived from have evolved to the present with a chondritic evolution. Adanac (b) and Adanac (c) have comparatively high $^{187}Re/^{188}Os$ as well, though not as high as Rincon and Tigre.

Bulk Isotope Dilution Re-Os Isotopic Composition & Model Age						
Sample	Re (ppb)	Os (ppb)	$^{187}Os/^{188}Os$	$^{187}Re/^{188}Os$	γ Os (t)	Model Age (Ma)
Madrigal	1.03 ± 0.05	1.195 ± 0.002	0.1323 ± 0.0001	4.151 ± 0.208	4.0	N/A
Carate (c)	0.598 ± 0.030	1.635 ± 0.003	0.1329 ± 0.0001	1.764 ± 0.088	4.6	N/A
Carate (b)	N.D.	1.071 ± 0.002	0.6741 ± 0.0007	N.D.	N.D.	N.D.
Carate (a)	0.406 ± 0.020	0.9846 ± 0.0020	0.1312 ± 0.0001	1.989 ± 0.099	3.2	N/A
Rincon	9.63 ± 0.48	0.1370 ± 0.0003	0.3927 ± 0.0004	349.6 ± 17.5	3.0	43
Tigre	3.15 ± 0.16	0.03124 ± 0.00006	0.7317 ± 0.0007	519.9 ± 26.0	2.3	61
Adanac (c)	2.15 ± 0.11	1.323 ± 0.003	0.1315 ± 0.0001	7.832 ± 0.392	3.2	36
Adanac (b)	6.36 ± 0.32	0.6368 ± 0.001	0.1272 ± 0.0001	48.15 ± 2.41	0.1	0.30
Adanac (a)	3.77 ± 0.19	0.8567 ± 0.0017	0.1312 ± 0.0001	21.21 ± 1.06	2.5	12
Agujas	1.06 ± 0.05	5.794 ± 0.012	0.1335 ± 0.0001	0.8782 ± 0.0439	5.1	N/A

Table 15: Bulk Re-Os isotopic composition and model ages, t is defined as the presumed age of formation of the source rock which the nuggets are sourced from. The t value used to calculate γ Os for each nugget was 3 Ma, excluding Rincon (45 Ma), Tigre (69.5 Ma), and Adanac (b) (0.1 Ma). Re concentrations were collected via solution ICP-MS and Os concentrations were collected via TIMS. Carate (b) was under spiked for Re, therefore the data was not reported.

Discussion

Surface Concentration

From our initial major and trace element analyses we concluded that there are no PGE alloy inclusions within our gold nuggets. Though the absence of inclusions within the nuggets was not the only thing that the line analyses revealed. The surface line analyses gave much higher concentrations of HSE than the spot analyses. During the line analysis, material is sampled only from the top micron or so of material whereas during spot analysis, tens of microns deep of material is sampled. The number of counts of the trace elements drop sharply during the ablation so these observations can most easily be reconciled if there is a thin, micron thick surficial layer of enrichment on the surface of the nuggets. Given that we were using the LA-ICP-MS data to determine the amount of nugget we needed to dissolve to get measurable amounts of osmium in our TIMS analyses, this was an important observation on the path to determining osmium concentrations in the samples. The surface concentration was also corroborated by the solution ICP-MS results, indicating that the surface of the nuggets was enriched with HSEs. For the bulk analyses, the nuggets were not leached. The surface may be enriched with HSEs, but not enough such that it would meaningfully change the measured bulk concentrations (Table 5 & Table 6).

Osmium Isotopic Composition

The TIMS analyses have yielded a wide spread of $^{187}Os/^{188}Os$ ratios, some radiogenic and some closer to that of the mantle. Of the nuggets analyzed in this study, Madrigal, Carate (a), Carate (c), Adanac (a), Adanac (b), Adanac (c) and Agujas all had $^{187}Os/^{188}Os$ ratios similar to that of the mantle (within 10% of the projected mantle average: 0.127), and excluding Adanac (a) and Adanac (b), these nuggets had comparatively low $^{187}Re/^{188}Os$ ratios (all below 10).

If these nuggets were to be sourced from a crustal rock, such as basalt, we would expect to see much higher $^{187}Os/^{188}Os$ and $^{187}Re/^{188}Os$ ratios. An isochron has been plotted to illustrate the Os and Re isotopic composition of the nuggets (Figure 7. And Figure 8.), assuming an initial $^{187}Os/^{188}Os$ of 1.3, with 88.5 Ma, 63 Ma and 43 Ma aged rocks (all within the age range of the Nicoya complex). The seven

nuggets with mantle-like ratios of $^{187}Os/^{188}Os$ have comparatively low $^{187}Re/^{188}Os$ ratios. Because of this, these nuggets would have to be sourced from a young mafic rock such as basalt (< 10 Ma).

The Nicoya complex has been interpreted to be an ophiolite complex, meaning that although no exposed ultramafic rocks have been discovered, there are likely either undocumented or unexposed ultramafic rocks underlying the mafic rocks. Madrigal, Carate (a), Carate (c) and Agujas all have $^{187}Os/^{188}Os$ and $^{187}Re/^{188}Os$ ratios indicating that if the nuggets were to be sourced from a more evolved mafic rock, such as a basalt, they would need to be younger than 10 million years old. This is in direct contrast to the age of the Nicoya Complex (88.5-33.9 Ma), which is the reported source of native gold on the Osa peninsula (Berrange & Thorpe, 1988) as well as the youngest igneous rock that the gold could be sourced from on the Osa peninsula. Recent research into gabbros from the Gorgona Islands have yielded $^{187}Os/^{188}Os$ and $^{187}Re/^{188}Os$ ratios like those of our samples (Walker, 2020, personal communication) (Figure 8.). Gabbro is widely considered the coarse-grained equivalent of basalt, though the Gorgona island gabbros appear more like an ultramafic rock in terms of Os, meaning that the gabbros present on the Osa peninsula could be a plausible source of the gold nuggets.

The more complicated nuggets to decipher are those with non-mantle-like $^{187}Os/^{188}Os$ ratios. Carate (b) has a $^{187}Os/^{188}Os$ ratio of 0.674, Rincon has a $^{187}Os/^{188}Os$ ratio of 0.393 and Tigre with the highest ratio of 0.732. Regardless of having a radiogenic $^{187}Os/^{188}Os$ ratio, Rincon and Tigre are also likely sourced from a similar source lithology to Madrigal, Carate (a), Carate (c) and Agujas. Under the assumption that the precursor materials of which the nuggets are derived, evolved from a magma to the time they were emplaced on the crust with a chondritic evolution, they can be dated to have model ages of 43 million years for Rincon and 61 million years for Tigre (Figure 7.). This implies that the nuggets could feasibly be derived from a similar source lithology to the other Costa Rican nuggets. The only difference being which the material which the nuggets with more radiogenic ratios were derived from had to be emplaced in the crust 40 to 60 million years ago.

This information provides two major constraints for the 6 Costa Rican gold nuggets regarding their source lithology. Given that they are likely derived from the Nicoya Complex, the age of their source lithology is no older than 88.5 Ma and no younger than 33.9 Ma. Assuming that the osmium compositions in the nuggets reflect the composition of the source lithology, given their isotopic composition, the gold could not have been sourced from more evolved rocks such as basalts. Through process of elimination, this leaves two possible options for the source lithology of the gold nuggets, exposed gabbros, and possible unexposed or undocumented ultramafic material.

Regarding the British Columbian nuggets, Adanac (b) has a chondritic $^{187}Os/^{188}Os$ ratio (0.1272), but a comparatively high $^{187}Re/^{188}Os$, implying that the nugget formed in the past few million years, and has not had the time to grow substantial radiogenic ^{187}Os. As for Adanac (a) and Adanac (c), their $^{187}Os/^{188}Os$ ratios are non-radiogenic (0.1312 and 0.1315) and like Adanac (b), though to a lesser degree, their $^{187}Re/^{188}Os$ ratio indicates a fairly recent formation on a geologic timescale. This does not mean that the nuggets came from a young rock, only that the associated Re and Os were incorporated into the nugget in the past few million years. Because the Os isotopic compositions ($^{187}Os/^{188}Os$ ratio of 0.127) are not very radiogenic, their high $^{187}Re/^{188}Os$ ratios could have only been achieved by a comparatively recent formation of the nuggets. While the $^{187}Re/^{188}Os$ ratios are enriched compared to the other nuggets, they are still not high enough to indicate a more evolved mafic source lithology, given that the youngest evolved mafic rock in the Atlin area (47 Ma) is far too old for the $^{187}Os/^{188}Os$ ratios measured in the nuggets. Regarding the plutons in the Atlin area, the nuggets $^{187}Re/^{188}Os$ ratios are too low to indicate a felsic source lithology. Therefore, the most likely option for the source lithology of the British Columbian nuggets is the ultramafic rocks in the Cache Creek Group (298 Ma - 47 Ma).

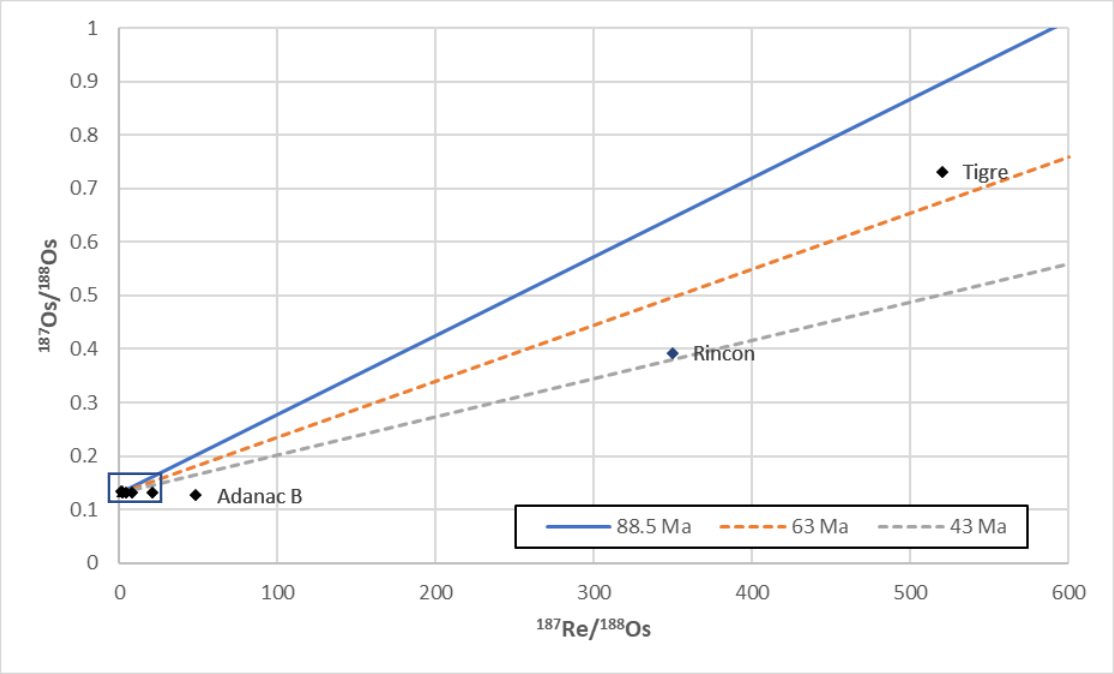

Figure 7: $^{187}Re/^{188}Os$ vs $^{187}Os/^{188}Os$ isochron figure. Projected $^{187}Re/^{188}Os$ and $^{187}Os/^{188}Os$ ratios of 88.5 Ma (blue line), 63 Ma (dashed orange line), and 43 Ma (dashed grey line) year old source rocks with estimated 0.13 initial $^{187}Os/^{188}Os$ ratios. The black box represents the data depicted in figure 6.

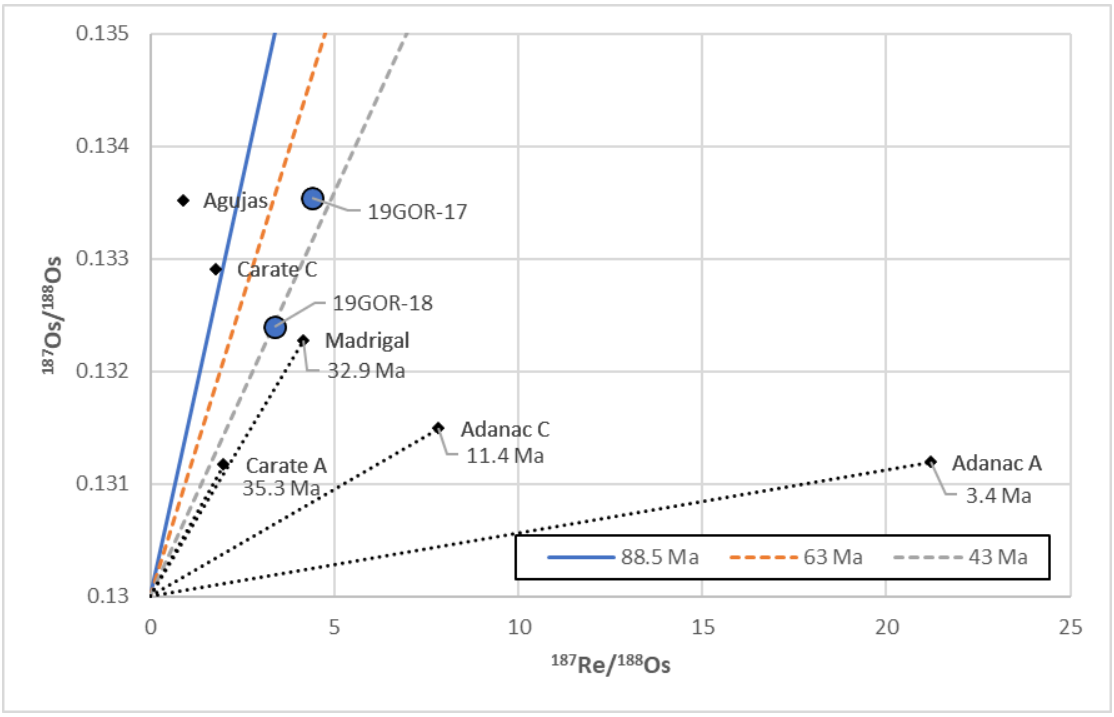

Figure 8: $^{187}Re/^{188}Os$ vs $^{187}Os/^{188}Os$ isochron figure, with the same projected ratios and ages of figure 6. Model ages of Madrigal, Carate (a), Adanac (c), and Adanac (a) have been calculated from the coordinates on the isochron and depicted in the figure. The blue circles in this figure depict Gorgona Island gabbros isotopic composition (Walker, 2020)

Summary

The goal of this study was to determine the source lithology of several gold nuggets from Costa Rica and British Columbia. Various theories as to how gold nuggets form have been proposed ranging from hydrothermal systems precipitating them out, to gold simply weathering out of ultramafic rock and being transported mechanically. Geochemical tracers are likely a feasible way to determine the source lithology of a given gold nugget. The ratio $^{187}Os/^{188}Os$ as well as siderophile element concentrations within a set of ten gold nuggets sourced from British Columbia and the Osa peninsula of Costa Rica were determined to assess this. The composition of the nuggets was measured via LA-ICP-MS, EPMA, and TIMS.

The samples have proven to be more complex than initially thought. This is in part due to a very thin layer on the surface of the nuggets enriched in HSEs. The nuggets have also proven to be difficult to analyze via LA-ICP-MS, solution ICP-MS and isotope dilution. LA-ICP-MS analyses were only usable as qualitative data due to low concentrations of siderophile elements and the lack of an adequate gold standard for internal and external standardization, meaning that the analyses would have intrinsically low accuracy. Spike weights were difficult to determine due to the lack of accuracy in LA-ICP-MS analyses which we were using as guidelines for spiking. This difficulty in spiking lead to over/under spiking of nuggets, making all Pt and several other HSE concentration measurements unusable. Regarding solution ICP-MS, Au interference with Ir and Pt measurements yielded multiple unusable Ir measurements and no useable Pt measurements.

Regardless of difficulties, the likely source lithology of nine of the ten nuggets were able to be determined. As expected, the nuggets had measurable amounts of Os. While many of the nuggets had $^{187}Os/^{188}Os$ ratios like that of the mantle, three of the nuggets had radiogenic $^{187}Os/^{188}Os$ ratios. Two of the Costa Rican nuggets had radiogenic $^{187}Os/^{188}Os$ ratios, though they had a feasible model age which implied that they were likely sourced from rock between 40 and 60 million years old. Meaning that they still fell within the age range of the Nicoya Complex on the Osa peninsula.

Six of the seven Costa Rican nuggets are plausibly derived from ultramafic rocks, though there are no exposed ultramafic rocks in the Nicoya Complex, or the Osa Peninsula as a whole. Considering that the Nicoya Complex is an ophiolite complex, this does not mean that ultramafic rocks are not present, only that they are unexposed or undocumented. If hydrothermal fluids are assumed to be the mechanism concentrating the gold from the source rock into nuggets, it is plausible that the gold was transported out of the unexposed ultramafic component of the Nicoya Complex into the overlying mafic rocks. Exposed gabbros in the Nicoya complex could also be a source lithology for 6 of the Costa Rican nuggets. This is because gabbros of similar age on the Gorgona Islands have been found to have similar Re-Os characteristics as these gold nuggets (Walker, 2020, personal communication) The provenance of the last Costa Rican nugget remains unknown. This is due to difficulties during spiking the nugget during isotope dilution, causing the Re data to be unusable. Due to Re being critical to this study, without adequate Re measurements, any conclusion made concerning the hypothesis regarding this nugget would be presumptuous at best.

The three British Columbian nuggets are plausibly derived from the ultramafic rock in the Cache Creek Group. This was determined due to the nuggets having non-radiogenic $^{187}Os/^{188}Os$ ratios, while having $^{187}Re/^{188}Os$ ratios too low to be associated with more evolved intrusive rocks.

Acknowledgements

The author would like to thank Dr. Richard Walker, Dr. Richard Ash, and Dr. Philip Piccoli for guidance in both the collection of data for this paper and writing the paper itself. The lessons this experience has provided are irreplaceable and I am incredibly grateful to be given the opportunity to work with such amazing mentors.

Honor Code

I pledge on my honor that I have not given or received any unauthorized assistance on this assignment.

References

Becker, H., Horan, M., Walker, R., Gao, S., Lorand, J., & Rudnick, R. (2006). Highly siderophile element composition of the Earth's primitive upper mantle: Constraints from new data on peridotite massifs and xenoliths. *Geochimica et Cosmochimica Acta, 70*(17), 4528-4550. doi:10.1016/j.gca.2006.06.004

Berrangé, J., & Thorpe, R. (1988). The geology, geochemistry and emplacement of the Cretaceous—Tertiary ophiolitic Nicoya Complex of the Osa Peninsula, southern Costa Rica. *Tectonophysics, 147*(3-4), 193-220. doi:10.1016/0040-1951(88)90187-4

Bushmin, S. A., Belyatsky, B. V., Krymsky, R. S., Glebovitskii, V. A., Buiko, A. K., Savva, E. V., & Sergeev, S. A. (2013). Isochron Re-Os age of gold from mayskoe gold-quartz vein deposit (Northern Karelia, Baltic Shield). *Doklady Earth Sciences, 448*(1), 54-57. doi:10.1134/s1028334x13010030

Fischer-Gödde, M., Becker, H., & Wombacher, F. (2011). Rhodium, gold and other highly siderophile elements in orogenic peridotites and peridotite xenoliths. *Chemical Geology, 280*(3-4), 365-383. doi:10.1016/j.chemgeo.2010.11.024

Hattori, K., & Cabri, L. (1992). Origin of platinum-group mineral nuggets inferred from an osmium-isotope study. The Canadian Mineralogist. 30. 289-301.

Jansen, M., Aulbach, S., Hauptmann, A., Höfer, H. E., Klein, S., Krüger, M., & Zettler, R. L. (2016). Platinum group placer minerals in ancient gold artifacts – Geochemistry and osmium isotopes of inclusions in Early Bronze Age gold from Ur/Mesopotamia. *Journal of Archaeological Science, 68*, 12-23. doi:10.1016/j.jas.2016.02.004

Junk, S. A., & Pernicka, E. (2003). An Assessment of Osmium Isotope Ratios as a New Tool to Determine the Provenance of Gold with Platinum-Group Metal Inclusions*. *Archaeometry, 45*(2), 313-331. doi:10.1111/1475-4754.00110

McDonough, W., & Sun, S. (1995). The composition of the Earth. *Chemical Geology, 120*(3-4), 223-253. doi:10.1016/0009-2541(94)00140-4

Pinsent R. (2006). Surficial Geology Report on the Adanac (Ruby Creek) Property; *Atlin Mining Division*

Rudnick, R. L., & Gao, S. (2004). The Composition of the Continental Crust. In *Treatise on geochemistry* (pp. 1-56). Oxford, UK: Elsevier Pergamon.

Shirey, S. B., & Walker, R. J. (1998). The Re-Os Isotope System in Cosmochemistry and High-Temperature Geochemistry. *Annual Reviews*.

Sisson, T. W. (2003). Native gold in a Hawaiian alkalic magma. *Economic Geology, 98*(3), 643-648. doi:10.2113/gsecongeo.98.3.643

Smith, J. L. (2009). A Study of the Adanac Porphyry Molybdenum Deposit and Surrounding placer Gold Mineralization in Northwest British Columbia With a Comparison to Porphyry Molybdenum Deposits in the North American Cordillera and Igneous Geochemistry of the Western United States. *University of Nevada, Reno*.

U.S. Geological Survey, 2020, Geology and resource assessment of Costa Rica. (n.d.). Retrieved November 16, 2020, from https://mrdata.usgs.gov/dds-19/

Walker, R. J., Bohlke, J. K., McDonough, W. F., & Li, J. (2007). Effects of Mother Lode-Type Gold Mineralization on 187Os/188Os and Platinum Group Element Concentrations in Peridotite: Alleghany District, California. *Economic Geology, 102*(6), 1079-1089. doi:10.2113/gsecongeo.102.6.1079

Walker, R. J., Storey, M., Kerr, A. C., Tarney, J., & Arndt, N. T. (1999). Implications of 187Os isotopic heterogeneities in a mantle plume: Evidence from Gorgona Island and Curaçao. *Geochimica Et Cosmochimica Acta, 63*(5), 713-728. doi:10.1016/s0016-7037(99)00041-1

Youngson, J., & Craw, D. (1992). Gold nugget growth during tectonically induced sedimentary recycling, Otago, New Zealand. *Sedimentary Geology, 84*(1-4), 71-88. doi:10.1016/0037-0738(93)90046-8

Zhu, Y., An, F., & Tan, J. (2011). Geochemistry of hydrothermal gold deposits: A review,. *Geoscience Frontiers, 2*(3), 367-374. doi:10.1016/j.gsf.2011.05.006